eNeuro

Research Article: New Research
Sensory and Motor Systems

Neural Encoding of Direction and Distance across Reference Frames in Visually Guided Reaching

Alejandra Harris Caceres,[1]* Deborah A. Barany,[2,3]* Neil M. Dundon,[4,5] Jolinda Smith,[1] and Michelle Marneweck[1,6,7]

[1]Department of Human Physiology, University of Oregon, Eugene, Oregon 97403, [2]Department of Kinesiology, University of Georgia, Athens, Georgia 30602, [3]Department of Interdisciplinary Biomedical Sciences, School of Medicine, University of Georgia, Athens, Georgia 30606, [4]Department of Psychological and Brain Sciences, University of California Santa Barbara, Santa Barbara, California 93106, [5]Department of Child and Adolescent Psychiatry, Psychotherapy and Psychosomatics, University of Freiburg, Freiburg 79104, Germany, [6]Institute of Neuroscience, University of Oregon, Eugene, Oregon 97403, and [7]Phil and Penny Knight Campus for Accelerating Scientific Impact, Eugene, Oregon 97403

Abstract

Goal-directed actions require transforming sensory information into motor plans defined across multiple parameters and reference frames. Substantial evidence supports the encoding of target direction in gaze- and body-centered coordinates within parietal and premotor regions. However, how the brain encodes the equally critical parameter of target distance remains less understood. Here, using Bayesian pattern component modeling of fMRI data during a delayed reach-to-target task, we dissociated the neural encoding of both target direction and the relative distances between target, gaze, and hand at early and late stages of motor planning. This approach revealed independent representations of direction and distance along the human dorsomedial reach pathway. During early planning, most premotor and superior parietal areas encoded a target's distance in single or multiple reference frames and encoded its direction. In contrast, distance encoding was magnified in gaze- and body-centric reference frames during late planning. These results emphasize a flexible and efficient human central nervous system that achieves goals by remapping sensory information related to multiple parameters, such as distance and direction, in the same brain areas.

Key words: fMRI; goal-directed action; motor planning; reaching; reference frames; representational similarity analyses; sensorimotor transformation

Significance Statement

Motor plans specify various parameters, e.g., target direction and distance, each of which can be defined in multiple reference frames relative to gaze, limb, or head. Combining fMRI, a delayed reach-to-target task, and Bayesian pattern component modeling, we present evidence for independent goal-relevant representations of direction and distance in multiple reference frames across early and late planning along the dorsomedial reach pathway. Initially, areas encoding distance also encode direction, but later in planning, distance encoding in multiple reference frames was magnified. These results emphasize central nervous system flexibility in transforming movement parameters in multiple reference frames crucial for successful goal-directed actions and have important implications for brain–computer interface technology advances with sensory integration.

Received Sept. 16, 2024; revised Oct. 19, 2024; accepted Nov. 6, 2024.

The authors declare no competing financial interests.

Author contributions: D.A.B., N.M.D., J.S., and M.M. designed research; A.H.C. and M.M. performed research; A.H.C., D.A.B., N.M.D., and M.M. analyzed data; A.H.C., D.A.B., N.M.D., J.S., and M.M. wrote the paper.

This work was supported by the Wu Tsai Human Performance Alliance and the Joe and Clara Tsai Foundation. We thank David Badcock for his help with visual angle and acuity considerations, Scott T. Grafton and Giacomo Ariani for their helpful input on data analyses and interpretation, and Mark M. Churchland for his help with interpretation. We thank Nicole Stoehr and Suhana Ahamed for assisting with developing and piloting the task design and Kaden Coulter for assisting with analyses.

Continued on next page.

Introduction

Visual goal-directed reaching relies on neuronal events that transform visual information about a target location into an actionable plan to move the chosen effector (Crawford

et al., 2011; Fooken et al., 2023). Achieving a motor goal necessitates specifying not just the direction, but also the distance to the target. Complexity arises because parameters can be specified in multiple reference frames relative to the gaze, head, or limb (Pouget et al., 2002; Battaglia-Mayer et al., 2003; Fiehler and Karimpur, 2023). While direction has been extensively studied, how the brain encodes distance remains less understood. Determining how the brain supports these sensorimotor transformations is an urgent challenge considering the gains in robotic control with brain–computer interface technology integrating sensory information (Flesher et al., 2021).

A substantial body of research has demonstrated that encoding movement parameters in multiple coordinate frames provides the flexibility and efficiency needed for optimal sensorimotor transformations; however, this has been primarily studied in relation to target direction. Monkey electrophysiology studies and human functional neuroimaging, neurostimulation, and lesion studies have identified the superior parietal cortex (SPL) and dorsal premotor cortex (PMd) as critical nodes for computing reaching actions (Wise and Mauritz, 1985; Kalaska and Crammond, 1995; Galletti et al., 1997; Graziano and Gross, 1998; Crammond and Kalaska, 2000; Andersen and Buneo, 2002; Bastian et al., 2003; Johnson and Grafton, 2003; Rizzolatti and Matelli, 2003; Gallivan et al., 2009; Pisella et al., 2009; Fabbri et al., 2010; Kaufman et al., 2010; Gallivan et al., 2011a,b; Davare et al., 2012; Barany et al., 2014; Fabbri et al., 2014; Kaufman et al., 2014; Coallier et al., 2015). SPL and PMd encode a target's direction in body- and gaze-centric reference frames often via overlapping neuronal populations within this dorsomedial reach stream (Boussaoud et al., 1998; Buneo et al., 2002; Batista et al., 2007; Marzocchi et al., 2008; Bernier and Grafton, 2010; Beurze et al., 2010; Chang and Snyder, 2010; Bremner and Andersen, 2012; Hadjidimitrakis et al., 2014a; Leoné et al., 2015; Bosco et al., 2016; Piserchia et al., 2016; Cappadocia et al., 2017; De Vitis et al., 2019; Magri et al., 2019). Encoding target direction in multiple frames supports computational models that emphasize the flexibility, efficiency, and power of individual nodes to optimally transform between extrinsic or intrinsic inputs (Körding and Wolpert, 2004; Sober and Sabes, 2005; McGuire and Sabes, 2009).

Despite its equally critical role in successful reaching, much less is known about how the brain encodes target distance. Behavioral studies suggest that direction and distance are specified independently (Gordon et al., 1994; Messier and Kalaska, 1997; Vindras et al., 2005). There is a growing number of datasets on nonhuman primates showing distance, like direction, is encoded in multiple reference frames (Hadjidimitrakis et al., 2014a, 2017, 2020; Bosco et al., 2016; Piserchia et al., 2016; De Vitis et al., 2019) and processed after direction in PMd (Messier and Kalaska, 2000; Churchland et al., 2006a; Davare et al., 2015) and SPL (Hadjidimitrakis et al., 2014b, 2022). In humans, transcranial magnetic stimulation of SPL before movement onset resulted in directional errors, whereas PMd stimulation at a slightly later time point disrupted accurate computations of movement distance, supporting serial processing of direction, and then distance (Davare et al., 2015). During movement execution, SPL and PMd represent both distance and direction features (Fabbri et al., 2012). These similarities—including independent specification, serial processing, neural overlap, and shared susceptibility to disruption—suggest that distance, like direction, may also have a flexible representation across multiple reference frames. However, the coordinate frame(s) in which distance is planned is unknown, especially in humans.

The primary aim of this study was to determine the reference frame in which a target's distance is represented in the human dorsomedial reach pathway during early and late planning of an upcoming motor action. One hypothesis is that, unlike direction, a target's distance is encoded strictly within a single reference frame, reflecting a hierarchical cost-efficient strategy where only some movement parameters (i.e., direction) but not all (i.e., distance) undergo sensorimotor transformations (Turella et al., 2020). Alternatively, distance might be encoded in multiple reference frames, similar to direction (Bosco et al., 2016), which suggests a similar circuitry that flexibly transforms between gaze and body-centered coordinate spaces for distance as it does for direction. We also aimed to investigate whether distance representations become more pronounced during later stages of planning, in line with serial processing accounts.

To address these questions, we employed fMRI with a delayed reach-to-target task, varying the distance (near vs far) between target and gaze, target and hand, and gaze and hand, as well as the direction (left vs right) of the target, gaze, and hand positions

*A.H.C. and D.A.B. contributed equally to this work.

Correspondence should be addressed to Michelle Marneweck at mmar@uoregon.edu.

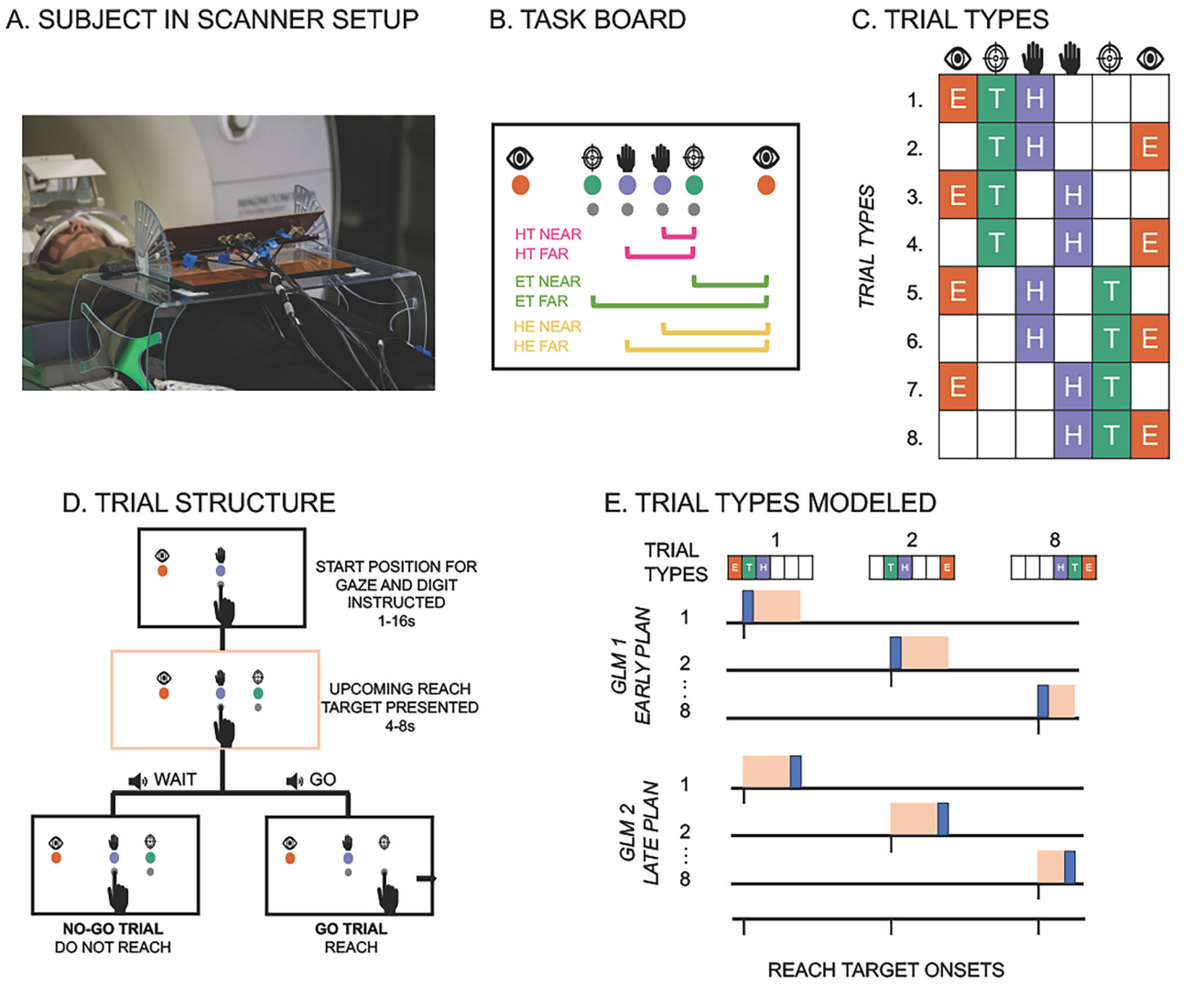

Figure 1. ***A***, Participants performed a reach-to-target task with their right hand on an interactive task board during fMRI. A mirror attached to the head coil allowed seeing the task board and their hand as if looking directly at it. ***B***, Schematic of the reach-to-target task board. Colored LEDs and icons showed hand, target, and gaze positions and two buttons for hand and target positions, respectively. Near and far vector distances between eye gaze and target (ET), hand and target (HT), and between hand and eye gaze (HE) are visualized but not present on the actual board. ***C***, Eight task trial types with eye gaze (E), initial hand (H), and target (T) position on the left or right side of the board gave two possible target, gaze, and hand position directions (left vs right) and two possible distances (near vs far) between target and eye gaze, target and hand, and gaze and hand. ***D***, Each trial started with a hand and gaze position instructed, followed by the appearance of a goal target, after which an audio cue instructed a go or a no-go trial. No-go trials were used for analyses to prevent movement execution contamination in early and late plan-related BOLD activity. ***E***, General linear model (GLM) structures where each GLM models the extent to which a trial type predicts BOLD activity during either the early (first 2 s) or late planning (last 2 s) period during which an upcoming target is presented. The resultant beta-estimates then serve as inputs to variational representational analysis (vRSA) of fMRI data to test the extent to which a region of interest represents features or components such as a target, gaze, or hand direction, or the distance between each of these during early and late planning.

(Fig. 1). Using variational representational analysis (vRSA) implementing Bayesian pattern component modeling of fMRI data (Friston et al., 2019; Marneweck et al., 2023; Kreter et al., 2024), we determined how distance and direction parameters are represented in SPL, PMd, and primary motor cortex (M1) during early and late planning. Our results show that during early planning, some regions encoded target distance in a single reference frame, mostly gaze-centric, while other areas represented this information in multiple reference frames. Notably, all regions encoding distance information also encoded direction information independently. During late planning, consistent with serial processing accounts, distance representational specificity in multiple reference frames magnified across the dorsomedial reach pathway. These findings demonstrate how and when multiple goal-relevant representations are specified in humans, supporting the hypothesis that similar circuitry flexibly transforms between gaze- and body-centered coordinate spaces for distance as it does for direction.

Materials and Methods

Participants

Twenty-seven right-handed young adults with normal or corrected-to-normal vision participated in this study (14 female, $M = 21.1 \pm 3.3$ years). All participants reported having no history of neurological or neuromuscular diagnoses and no motor or cognitive impairments that would adversely affect their ability to perform motor tasks. All participants gave written informed consent, and the experimental procedures were approved by the University of Oregon Institutional Review Board.

Materials, design, and procedure

Materials. An interactive task board was held by a stand 4 cm above the table and angled 40.6° relative to the table, which piloting showed as an optimal orientation for full view (Fig. 1*A*). As shown in Figure 1*B*, the task board base (width, 40.0 cm; length, 10.0 cm; depth, 6.5 cm) consisted of six colored LEDs that, when illuminated, would instruct a left- or right-sided gaze position (red), initial hand position (green), and target position (blue), respectively (we ensured all participants could discriminate between these colors before scanning). Four buttons to be pressed when instructed were positioned below each of the hand and target position LEDs. Icons illustrating the eye, hand, and target position were placed above each of the LEDs. The two hand LEDs were 2.3 cm apart and positioned in the middle of the board. On each of the outer sides of these hand LEDs 2.3 cm away were two target LEDs positioned 6.9 cm apart from each other. The gaze LEDs were 32.9 cm apart and positioned on the outer sides of the target LEDs.

The configuration of gaze, hand, and target positions on the task board gave two possible distances between eye gaze and target (ET near, 13.0 cm; ET far, 19.9 cm) and hand and target (HT near, 2.3 cm; HT far, 4.6 cm). Visual angles between gaze position and targets for ET-near and ET-far trials were 11.3 and 16.8°, respectively (from the distance of the bridge of the nose to the center of task board LEDs based on data from CDC-defined average height of females and males). Distances were selected to minimize visual acuity differences between ET near and far such that targets in both cases fell within an observer's 5–20° near-peripheral zone within which there are little changes in the parameters of acuity (Millodot et al., 1975; Larson and Loschky, 2009).

Eye tracking was performed outside the scanner with Pupil Core glasses and the head secured in a headrest, with an eye camera resolution and frequency of 192 × 192 pixels and 200 Hz, and a scene camera resolution and frame rate of 1,280 × 720 and 30 Hz (Kassner et al., 2014).

Anatomical and fMRI data were collected using a Siemens 3T Skyra (32-channel phased-array head coil). High-resolution 1 mm isotropic T1-weighted (TR, 2,500 ms; TE, 2.98 ms; FA, 7°; FOV, 256 mm) and T2*-weighted (TR, 3,200 ms; TE, 565 ms; FOV, 256 mm) images were acquired of the whole brain. Both sequences used volumetric navigators for prospective motion correction and selective reacquisition (Casey et al., 2018). Next, as subjects performed the reach-to-target task, BOLD contrast was measured with a multiband T2*-weighted echoplanar gradient echo imaging sequence (TR, 450 ms; TE, 30 ms; FA, 45°; FOV, 192 mm; multiband factor, 6). Each functional image consisted of 48 slices acquired parallel to the AC–PC plane (3 mm thick; 3 × 3 mm in-plane resolution; Moeller et al., 2010; Setsompop et al., 2012).

Experimental design and procedure. During fMRI, participants performed the reach-to-target task with their right hand on a task board at arm's length sitting on a marked spot on a table positioned over the hips of the subject. With a mirror attached to the head coil, subjects saw the task board and their hand (statically and during movement) as if they looked directly at it when sitting upright (Fig. 1*A*).

Participants reached to left- or right-sided targets, with initial hand position and gaze fixated in one of two locations, respectively (Fig. 1*B*,*C*). As seen in Figure 1*D*, each trial began with illuminated LEDs that instructed an initial hand position and a gaze position to focus on for the entire trial, which piloting showed were successfully adhered to (Table 1). After a variable delay period (1, 2, 4, 8, 16 s with the respective proportions of trials, [0.52, 0.26, 0.13, 0.06, 0.03]), a target LED illuminated for 4, 6, or 8 s (with the respective proportions of trials [0.56, 0.30, 0.14]). Next, an audio cue played through headphones indicating whether to perform the planned reach to target (i.e., "go," 60% of the trials) or not (i.e., "wait," 40% of the trials). The initial hand position and target position LEDs were turned off concurrently with the go/no-go cue to encourage planning the reach during this variable delay period during which the target was illuminated (Ariani et al., 2022). Feedback audio cues indicating success or error played after a correct or incorrect reach to the target or 2.5 s after the go/no-go cue if no movement was made with an additional 1 s interval between the feedback cue and the start of the next trial. There were eight trial types with two possible initial hand, target, and gaze positions, with the vector distance

Table 1. Percent time, in a given trial, in maintaining gaze within a predefined surrounding boundary organized by each combination of left- (L) and right-sided (R) gaze (E), initial hand (H), and target (T) position in two participants

H-T-E	L-R-L	L-*R*-R	L-L-R	R-R-R	R-L-R	R-L-L	L-L-L	R-R-L
Subj. 1	97.4	100.0	100.0	99.5	94.5	100.0	99.2	100
Subj. 2	99.6	99.4	99.8	98.8	100.0	99.6	100.0	100.0

between the gaze and target, hand and target, and hand and gaze varied in one of two ways (near vs far; Fig. 1*C*). After standardized instructions and 20 practice trials, participants completed six functional runs of 40 trials (five trials for each of the eight trial types). Stimulus and button press timings for each trial were controlled by a custom Python script.

The order and distribution of each of the eight trial types, go and no-go trials, and within-trial variable durations (delay and plan phases) was determined with the goal of minimizing the variance inflation factor (VIF) for each functional run (Ariani et al., 2022); VIF = var(E)/var(X), where var(E) is the mean estimation variance of all the regressor weights and var(X) the mean estimation variance had these regressors been estimated in isolation. VIF estimates the severity of multicollinearity between model regressors by providing an index of how much the variance of an estimated regression coefficient is increased because of collinearity. Large VIF values indicate regressors are not independent of each other, whereas a VIF of 1 means no inflation of variance between regressors. We optimized the design such that the VIF was below 1.15, indicating the independence of regressors. In addition, no evidence of multicollinearity was confirmed post data collection.

Hand and eye movement tracking. Reaction time and reach velocity were calculated for every go trial during scanning. Reaction time was calculated as the difference between the time from the go cue to when the hand released the initial hand position button. Reach velocity was calculated as the time from the initial hand position button release to a target button press given the distance traveled between the initial hand position and the target position. Pilot eye tracking data ($n = 2$) outside the MR with the head secured in a headrest during a 40-trial run showed high task adherence to gaze instruction (Table 1). Pupil Player software (v3.5.1) calculated gaze accuracy, defined as the mean distance difference in the visual angle of the fixation location and instructed gaze location. Mean gaze estimation is reported with an accuracy of 0.6° with 0.08° of precision (Kassner et al., 2014). Raw data was filtered to exclude blinks and recorded values with a confidence level below 0.6. Both subjects maintained gaze within a 3.5×3.5 cm boundary surrounding each illuminated gaze LED for each trial, in all combinations of gaze, target, and hand positions ($p > 0.05$; Table 1).

MRI preprocessing and statistical analyses. Functional images across runs were spatially realigned to a mean EPI image using a second-degree B-spline interpolation, coregistered to each individual subject's T1, and normalized between-subjects using SPM (fil.ion.ucl.ac.uk/spm). Head motion mean rotations and translations (with minimum and maximum values in parentheses) were minimal: *x*, 0.02 mm (−2.2, 2.02); *y*, 0.1 mm (−1.6, 3.3); *z*, 0.2 mm (−3.9, 4.2); pitch, −0.001 (−0.2, 0.1); roll, 0.0008 (−0.04, 0.03); yaw, 0.0008 (−0.04, 0.04).

Following preprocessing of fMRI data, we used vRSA (Friston et al., 2019; Marneweck and Grafton, 2020a,b,c; Marneweck et al., 2023; Kreter et al., 2024) with an adaptation to the MATLAB script DEMO_CVA_RSA.m available in SPM12. First, we estimated convolution-based GLMs in SPM12 for each subject and functional run separately with the Robust WLS Toolbox selected to down weight volumes with high noise variance to account for movement artifact (Diedrichsen and Shadmehr, 2005). We generated GLMs that estimated the extent to which planning a reach-to-target predicted BOLD activity for each of the eight trial types on no-go trials and on go trials (Fig. 1*E*). Planning was modeled during 2 s epochs with onsets marked at target presentation (i.e., early plan epoch) and during the last 2 s before the go/no-go cue (i.e., late plan epoch). Similar to several recent fMRI studies on motor planning, our analyses focused on no-go trials to prevent contamination of movement execution in GLM-derived estimates of activity during the planning phase (Ariani et al., 2018, 2022; Yewbrey et al., 2023). Planning of go trials, movement on each trial, and error trials (if any were made) were modeled as regressors of no interest and not used in further analyses.

Following the GLM step, we extracted GLM-derived beta values in primary motor, dorsal premotor, and superior parietal regions (Fig. 2) from the Julich Brain Atlas (Amunts et al., 2020) and from the Human Brainnetome Atlas (Fan et al., 2016) using FSL's fslmeants for each participant and functional run. The dorsal premotor area in the Julich atlas is subdivided cytoarchitectonically into three regions (6d1, 6d2, 6d3) in a rostrocaudal arrangement: 6d1 is the most caudal area, located on the precentral gyrus and a caudal part of the superior frontal gyrus (analogous to Glasser atlas area 6d; Glasser et al., 2016). 6d2 is located rostrally to 6d1 on the superior frontal gyrus (analogous to Glasser atlas area 6a), and 6d3 is located exclusively in the superior central sulcus, mainly ventrally to 6d2 (analogous to Glasser atlas area 6a). Hereafter we refer to 6d1 as PMd caudal, 6d2 as PMd rostral, and 6d3 as PMd rostrosulcal. The location and extent of key superior parietal areas correspond with the same areas as that in the Glasser atlas (Glasser et al., 2016), including SPL 7a and SPL 5m. Additionally, Julich area SPL 7a comprises mIPS per the Glasser atlas and previous human neuroimaging work (Bernier and Grafton, 2010) and pIPS per Fabbri et al. (2012).

We populated a condition (i.e., eight)-by-voxel U matrix describing each condition's voxel activity pattern (calculated with the above GLM) from which we computed a condition-by-condition second-order similarity matrix (G) that describes the relationship between these activity patterns (i.e., 8×8 covariance matrix), where $G = UU^T$. Higher values in off-diagonal cells reflect higher pattern similarity between conditions.

Next, we tested hypotheses regarding the composition of these second-order statistics by inferring the contribution of "components" to the G covariance matrix. Figure 3 shows the components we included. Our main components of interest test the extent to which a region represents a target's distance to the hand and gaze, respectively, during early and late planning (Fig. 3*A*). We also include direction-specific components that varied in the task design, including target position (absolute or relative to hand/body), initial hand position (absolute or relative to body), gaze positions (absolute or relative to

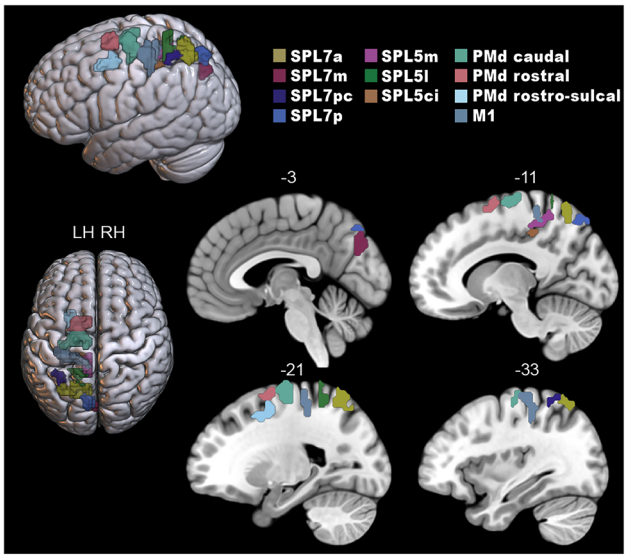

Figure 2. Predefined regions of interest extracted from the Julich Brain Atlas and Human Brainnetome atlas (primary motor cortex, M1) are displayed on the MNI-152 atlas using the visualization software, MRIcroGL. SPL, superior parietal; PMd, dorsal premotor.

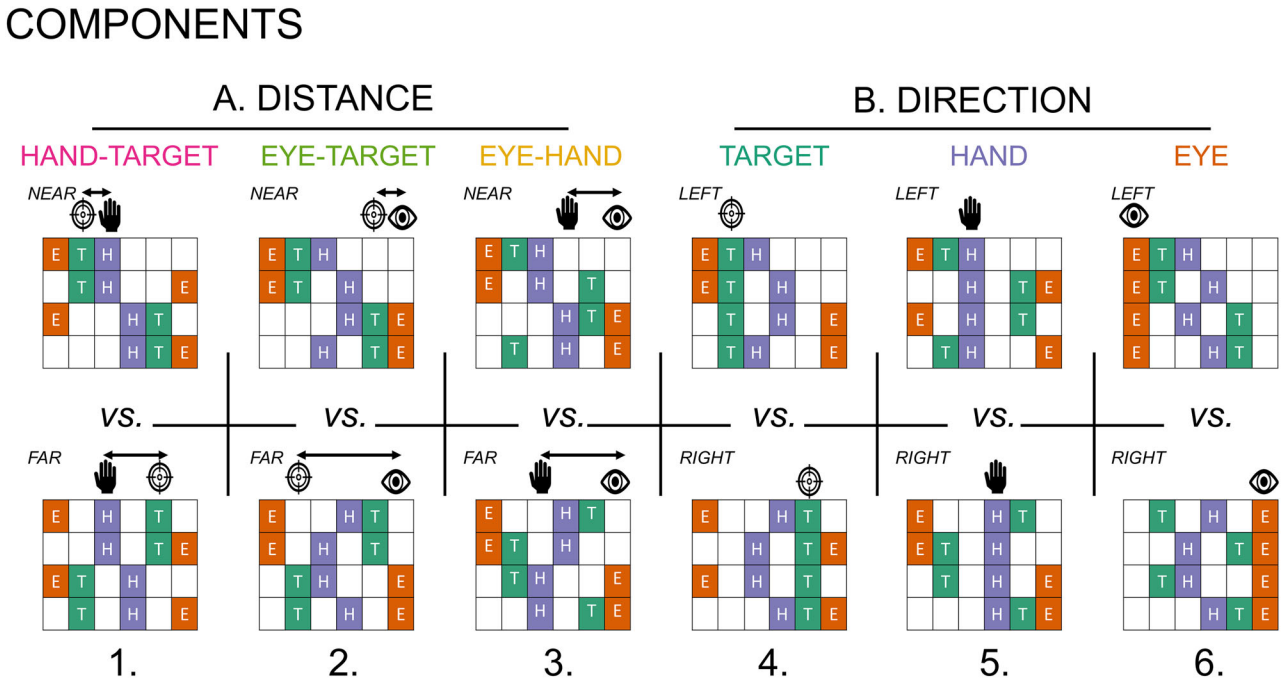

Figure 3. Variational representational similarity analysis (vRSA) implements Bayesian pattern component modeling of fMRI data tested for component effects of (***A***) the distance between (1) hand and target (HT), (2) eye gaze and target (ET), and (3) hand and eye gaze (HE), and (***B***) the direction of a (4) target position (T), (5) initial hand position (H), and (6) eye gaze position (E).

hand/body/target), and the hand–gaze distance, in each model (Fig. 3*B*). A strength of the vRSA approach is to test for the independent contribution of each component to the covariance G matrix (similar to multiple regression). The method quantifies the contribution of multiple components while taking into account all specific contrasts. In this way, a region of interest (ROI) can be sensitive to more than one component (i.e., such that a region's spatial activity patterns can represent multiple conditions of interest). Moreover, the covariance G matrix does not depend on the way columns of U are ordered (similar to a regression coefficient that will not change if shuffling the order of contributing pairwise *x*–*y* data). Pattern similarity can be identified even if not every column contributes to the covariance matrix.

Within this pattern component modeling framework, we could simultaneously test if and how distance between target, gaze, and hand position are represented, after accounting for direction components known to be encoded throughout this

network of regions (Wise and Mauritz, 1985; Kalaska and Crammond, 1995; Galletti et al., 1997; Graziano and Gross, 1998; Crammond and Kalaska, 2000; Andersen and Buneo, 2002; Bastian et al., 2003; Johnson and Grafton, 2003; Rizzolatti and Matelli, 2003; Gallivan et al., 2009; Pisella et al., 2009; Fabbri et al., 2010; Kaufman et al., 2010; Gallivan et al., 2011a,b; Davare et al., 2012; Barany et al., 2014; Fabbri et al., 2014; Kaufman et al., 2014; Coallier et al., 2015). Evidence of distance-based representations would be indicated by distinct activity between near versus far targets relative to (1) the initial hand position (HT), (2) the instructed eye gaze position (ET), and between near and far distances between the initial hand position and the instructed gaze position (HE). Evidence of direction-based representations would be indicated by distinct activity patterns of left- versus right-sided target (T), initial hand (H), and eye gaze (E) positions. We report vRSA results from GLM data modeling the 2 s at the start and the end of the planning epoch, respectively.

vRSA performed with SPM functions returns log evidence (marginal evidence) enumerating each component's contribution to the second-order matrix (G) for a given ROI at the group level, where more negative values are greater evidence of a component's contribution. To establish a criterion that sufficient evidence is observed, we take an ultraconservative step, detailed in Marneweck et al. (2023), by comparing actual log evidence with a null distribution of log evidence values for each component in each ROI. We derive each null distribution of log evidence by shuffling condition labels (not voxel order) in our U matrix 1,000 times, each time estimating G from the shuffled data and enumerating the component contributions. We can then illustrate the log evidence values of our real data (i.e., unshuffled) relative to these null distributions. We subtract the log evidence of the correct condition label from each of the shuffled log evidence values, creating a distribution of log Bayes factors, where higher values now communicate a strong effect. We conclude strongly credible effects only if there is little to no overlap between the null distribution and model evidence. We then formalize strong evidence for a component to contribute to a region's activity pattern if the real Bayes factor is three times more credible than the 80 or 95% strongest effect from the null distribution. Marneweck et al. (2023) for a comprehensive discussion on how this conservative approach mitigates the need for multiple comparison corrections within and across ROIs (also see (Gelman et al., 2012; Gelman and Loken, 2016; Krushke, 2014; Marneweck and Grafton, 2020c)).

Code accessibility. MATLAB code to run our modified vRSA with SPM functions can be found here: https://github.com/dundonnm/vRSAb.

Results

During fMRI, participants performed a delayed reach-to-target task, adapted from similar tasks used in nonhuman primates (Batista et al., 1999; Buneo et al., 2002; Pesaran et al., 2006; Batista et al., 2007), with two possible distances (near vs far) between hand and target, gaze and target, and gaze and hand and two possible directions (left vs right) for the target, gaze, and hand positions, respectively. The primary aim of this study was to determine if and how the distance of an upcoming reach target is represented in SPL, PMd, and M1 regions (Fig. 2) during early and late planning epochs. Secondarily, we determined if distance representations are magnified during later planning. Our analyses focused on plan periods of no-go trials to avoid movement execution contaminating plan-related BOLD activity (Ariani et al., 2022; Yewbrey et al., 2023).

Using vRSA of fMRI data (Friston et al., 2019; Marneweck and Grafton, 2020a,b,c; Marneweck et al., 2023) in predefined M1, PMd, and SPL ROIs, we determined the extent to which components of interest modulate overall condition-by-condition differences in neural activity patterns. We focused on six distinct components: distance between (1) hand and target, (2) gaze and target, and (3) hand and gaze and the direction of a (4) target, (5) initial hand position, and (6) gaze position (Fig. 3). The strength of the vRSA approach is that it tests for the independent contribution of each component to the condition-by-condition covariance matrix (similar to multiple regression). In this way, an ROI can be sensitive to more than one component (i.e., such that a region's spatial activity patterns can represent multiple conditions of interest).

Distance representations in single or multiple reference frames overlap with direction representations during early planning

We used vRSA to test for each hypothesized component's contribution to explaining the estimated spatial activity patterns for each condition and ROI during the first 2 s of planning. The vRSA returns log evidence enumerating the strength of each component's contribution to an ROI's activation pattern at the group level, with higher values indicating stronger effects (see Methods and Materials for details).

As seen in Figure 4, strong evidence of representations of a target's distance were present in multiple parietal (SPL 7a, 7pc, 5m, 5ci), dorsal premotor (PMd caudal, rostral, and rostral-sulcal), and M1 regions. Whereas SPL 7a, PMd rostral, and rostral-sulcal areas encoded target distance in both body- and gaze-centric reference frames (HT, ET), other regions encoded target distance in a single gaze-centric (M1, PMd caudal, SPL 5ci, 7pc) or body-centric reference frame (SPL 5m) during the early stages of planning. Most regions with activity patterns predicted by a target's distance also contained activity patterns predicted by target, hand, and eye gaze position direction-based components (T, H, and E) and the distance between hand and eye gaze position (HE). This suggests overlap in neuronal populations in SPL and PMd regions that encode direction and distance features critical for an upcoming goal-oriented reach. In addition, some parietal regions

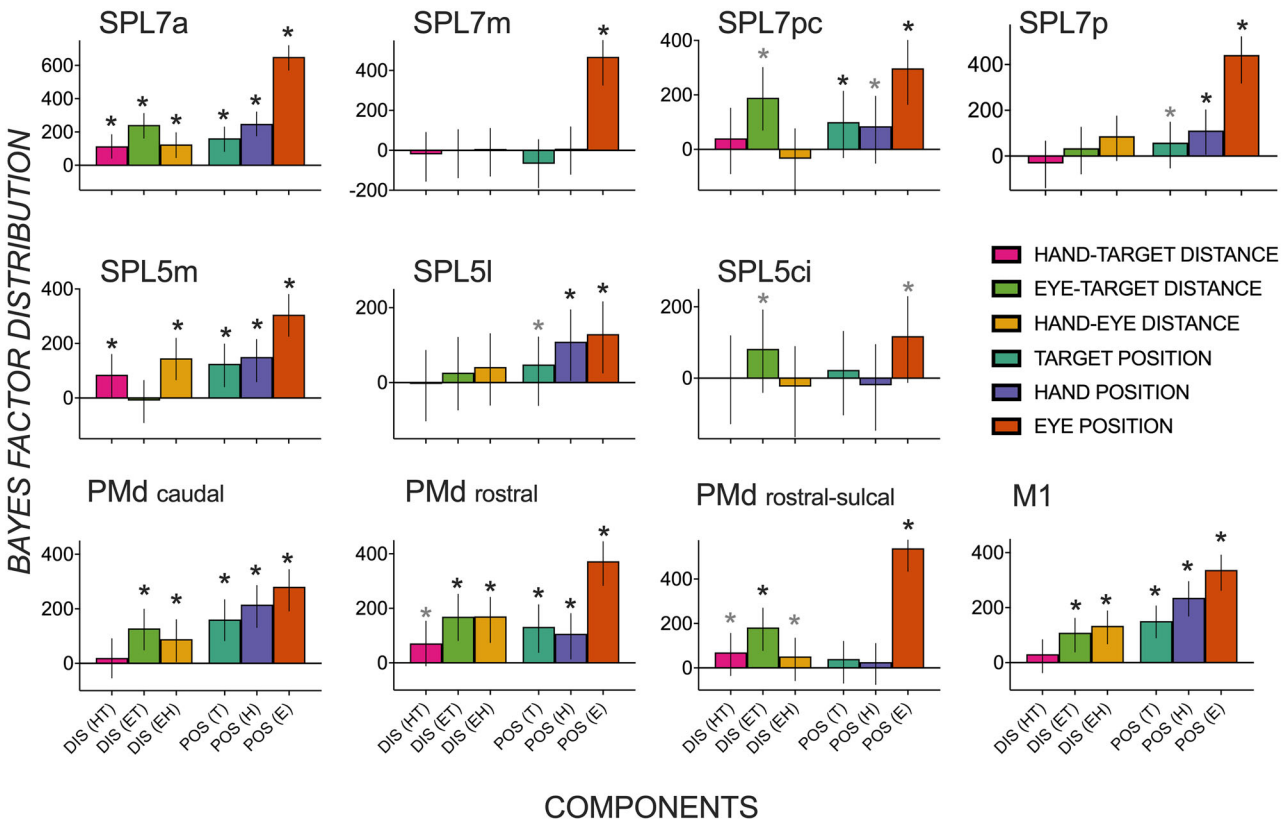

Figure 4. Distribution of Bayes factors (median and highest density interval as error bars) quantifying evidence for spatial activity patterns in dorsomedial reach regions during early planning to be predicted by an upcoming target's (1) body-centric distance—near versus far targets relative to the hand (HT); (2) gaze-centric distance—near versus far targets relative to the eye gaze (ET); (3) eye gaze–hand distance (EH); (4) target position—left versus right (T); (5) initial hand position—left versus right (H); (6) eye gaze position—left versus right (E). Components 1–3 test for distance-related effects, and components 4–6 test for direction-related effects. Asterisk (*) depicts substantial evidence for a component to contribute to a region's spatial activity pattern that is three times more credible than the 95% (black) or 80% (gray) strongest effect from a null distribution (i.e., shuffled condition labels). SPL, superior parietal; PMd, dorsal premotor; M1, primary motor; DIS, distance; POS, position.

represented direction components without distance features (SPL 7m, 7p, 5l), with effects for gaze position, indicating widespread direction-based effects. Overall, representational specificity for direction components dominated over that for distance during this early planning epoch, with far more credible effects for direction-based ($n = 27$) than distance-based ($n = 17$) components.

Heightened representational specificity of a target's distance during late planning

Figure 5 shows median Bayes factors quantifying the extent of credible evidence in each ROI for distance and direction-based effects during late planning. A striking observation is a growing number of ROIs encoding the target's distance in multiple reference frames alongside the relative dissipation of evidence of direction-based activity patterns. Representations of a target's distance in multiple gaze- and body-centered reference frames in early planning persist in late planning (SPL 7a, PMd rostral, PMd rostral-sulcal). Other regions previously shown to represent a target's distance in a single reference frame during early planning show evidence of body- and gaze-centric encoding during late planning (SPL 5m, PMd caudal, M1).

Surprisingly, direction-based representations were not as strong as in the early planning period. Multiple regions represented a target position or its direction relative to the hand/body in the early but not in the late phase of planning (SPL 7pc, 7p, 5m, PMd caudal, M1). Similarly, direction-based hand position representations observed during early planning were no longer credibly evident during late planning (SPL 7pc, 7p, 5m, PMd rostral). In contrast to direction-dominant encoding during early planning, credible effects consistent with magnified distance-representational specificity ($n = 21$) marginally exceeded direction-representational specificity ($n = 17$) across dorsomedial reach nodes.

Although direction-based representations relevant to an upcoming reach dissipated in late planning across the fronto-parietal network, they were not completely absent. Target position representations persisted in SPL 7a, 5l, and PMd rostral. Hand position representations were observed in SPL 7a, 5l, PMd caudal, and M1, and gaze position representations were seen in nearly all tested regions (except SPL 5ci).

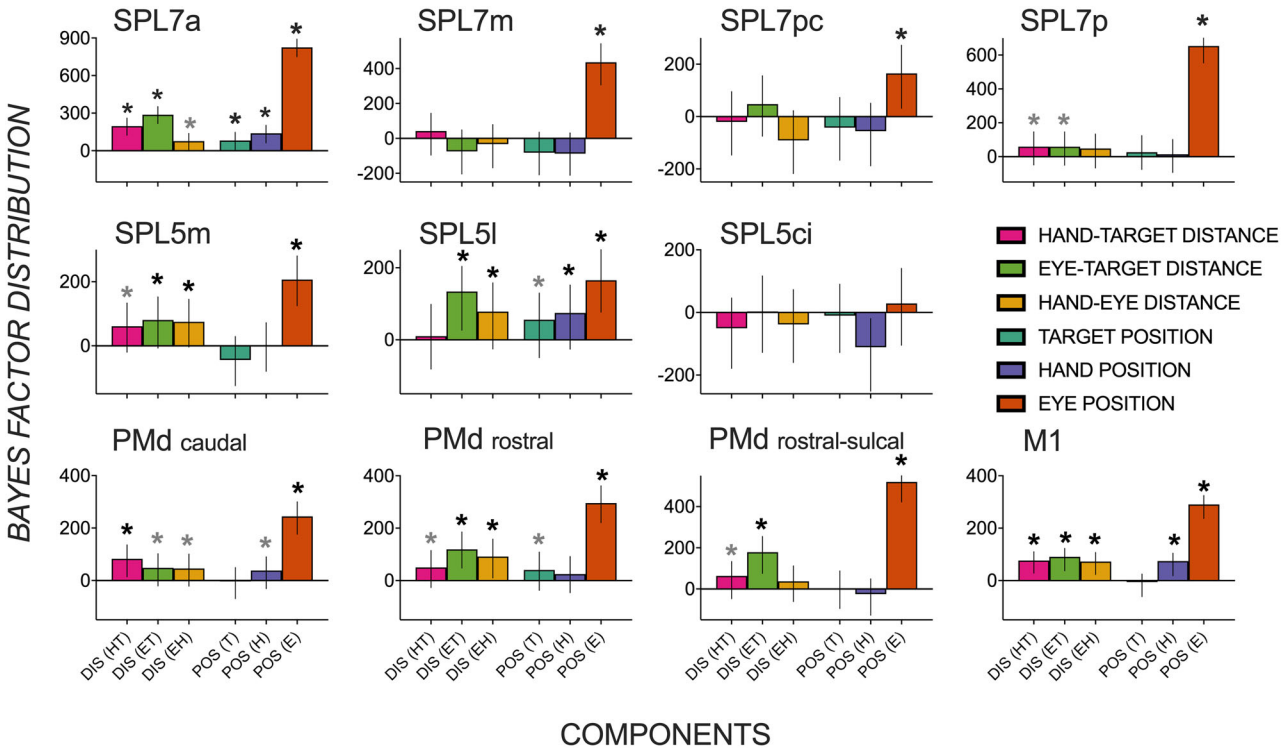

Figure 5. Distribution of Bayes factors (median and highest density interval as error bars) quantifying evidence for spatial activity patterns in dorsomedial reach regions during late planning to be predicted by an upcoming target's (1) body-centric distance—near versus far targets relative to the hand (HT); (2) gaze-centric distance—near versus far targets relative to the eye gaze (ET); (3) eye gaze–hand distance (EH); (4) target position—left versus right (T); (5) initial hand position—left versus right (H); (6) eye gaze position—left versus right (E). Asterisk (*) depicts substantial evidence for a component to contribute to a region's spatial activity pattern that is three times more credible than the 95% (black) or 80% (gray) strongest effect from a null distribution (i.e., shuffled condition labels). SPL, superior parietal; PMd, dorsal premotor; M1, primary motor; DIS, distance; POS, position.

Comparing go and no-go trial activity patterns

The go/no-go approach we adopted here has become an increasingly popular choice for isolating motor planning from execution in fMRI data (Cross et al., 2007; Ariani et al., 2018, 2022; Yewbrey et al., 2023). We nonetheless briefly report on spatial activity pattern differences between go and no-go trials in key regions revealed by our analyses of the planning period of no-go trials (SPL 7a, 5m, PMd caudal, rostral, rostral-sulcal, and M1). During early planning, we found no differences between go and no-go trials in any of these regions. During late planning, we only found differences in two motor regions (caudal PMd and M1) consistent with previous work (Denyer et al., 2022).

Activation pattern differences are not explained by behavioral differences

Figure 6 shows no significant differences in reaction time in initiating a reach and no differences in velocity in reaching for targets, with no significant main effects of components (gaze, hand, target, HT, ET, HE), contrasts (left vs right, near vs far), and no interactions (p's > 0.05). These behavioral measures were taken on go trials. However, they suggest that activity pattern differences reflecting representations of direction and distance during preparatory stages on a no-go trial found in our vRSA results are not predominantly a function of reaction time or velocity differences.

Discussion

Motivated by nonhuman primate electrophysiology studies (Batista et al., 1999, 2007; Buneo et al., 2002), we took a task-based fMRI approach exploiting pattern component modeling to determine how distance between target, gaze, and hand position are represented, while also accounting for direction components known to be encoded throughout the human dorsomedial reach pathway. During early planning, PMd rostral, PMd rostral-sulcal, and SPL 7a encoded target distance in multiple reference frames while other regions including M1, PMd caudal, and SPL 5m, 5ci, and 7pc encoded target distance in a single reference frame that was mostly gaze-centric (except SPL 5m). Notably, all regions encoding distance information also encoded direction information independently. Consistent with our hypothesis, during late planning, distance encoding in multiple reference frames was magnified. In addition, previously widespread direction-based effects were somewhat diminished during late relative to early planning. These results support the hypothesis that the

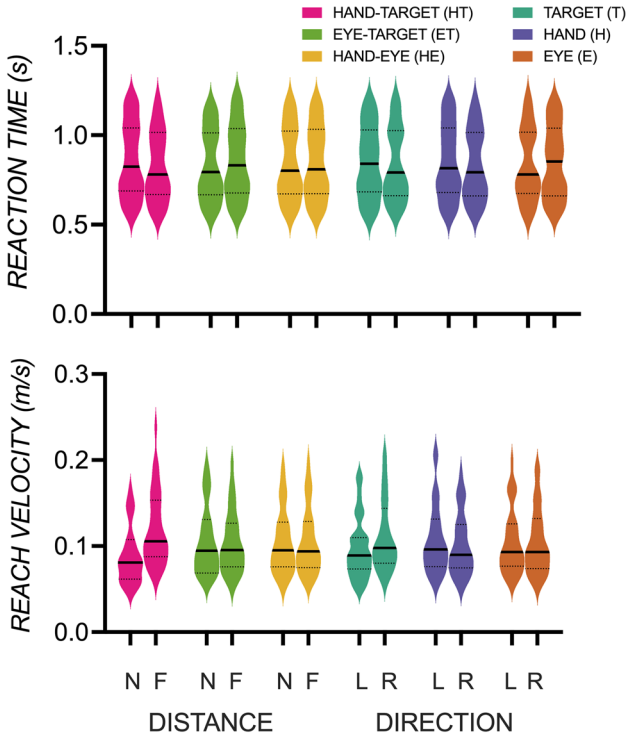

Figure 6. Reaction time (s) (top) and reach velocity (m/s) (bottom) were not significantly different between conditions contrasted in the vRSA of direction [left (L) vs right (R)] of eye gaze (E), hand (H), and target (T) and distance [near (N) vs far (F)] between hand and target (HT), eye gaze and target (ET), and hand and eye gaze (HE).

human central nervous system can flexibly define and transform movement-related parameters in multiple reference frames to enable successful goal-directed action.

A strength of the vRSA approach is to test for the independent contribution of each component to an overall spatial activity pattern while accounting for all included components. In this way, an ROI can be sensitive to more than one component. Mixed representations pose a greater challenge for winner-takes-all univariate methods or standard multivariate pattern decoding algorithms that assume representational singularity within a region (Dubois et al., 2015). Here we combined vRSA with a novel behavioral approach that not only dissociated distance and direction features but minimized between-condition activity pattern differences due to accuracy, speed, or visual acuity. With this approach, we derived strong empirical support for independent representations of distance and direction of an upcoming reach along the dorsomedial reach pathway.

Dorsomedial reach areas encoded a target's distance, demonstrating that parameters other than direction are specified by recruiting parietal and not just premotor regions (Fabbri et al., 2012). Findings in these regions and across epochs are generally consistent with the hypothesis that distance, like direction, is encoded in multiple reference frames. While we are the first study in humans to isolate and identify gaze- and body-centric distance representations across the dorsomedial reach pathway, independent of direction-based representations, our results align with a series of recent nonhuman primate studies showing mixed reference frame encoding in the medial sector of the posterior parietal cortex, i.e., SPL (Hadjidimitrakis et al., 2014a,b; Bosco et al., 2016; Piserchia et al., 2016; De Vitis et al., 2019; Hadjidimitrakis et al., 2022). Representations of distance in multiple reference frames suggest a similar circuitry that flexibly transforms between gaze- and body-centered coordinate spaces for distance as it does for direction.

Consistent with our hypotheses, distance representations in multiple reference frames were magnified during later planning. During early planning, SPL 7a, PMd rostral, and PMd rostral-sulcal regions represented distance in multiple reference frames. Other regions (SPL 7pc, 5ci, PMd caudal, M1) only represented gaze-centric distance, whereas somatosensory SPL 5m represented target distance in body coordinates. In late planning, all regions with credible evidence represented target distance in body- and gaze-centered coordinates (SPL 7a, 7p, 5m, PMd caudal, rostral, rostral-sulcal, M1). Gaze-centric representations during early planning and body-centric distance representations that were only observed in late planning (e.g., PMd caudal, M1) are consistent with nonhuman primate work showing the encoding of target parameters in gaze-centric preceding body-centric reference frames (Bremner and Andersen, 2012; Cappadocia et al., 2017). Intriguingly, SPL 5m represented the target distance in only a body-centric reference frame in early planning and then in both body- and gaze-centric reference frames in late planning, suggesting that gaze-centric need not always precede body-centric representations. These results provide empirical support for fluidity in how and when a region represents

target distance, with increasing support for spatial overlap in parametric representations of an upcoming target in multiple frames (Boussaoud et al., 1998; Buneo et al., 2002; Batista et al., 2007; Marzocchi et al., 2008; Bernier and Grafton, 2010; Beurze et al., 2010; Chang and Snyder, 2010; Bremner and Andersen, 2012; Hadjidimitrakis et al., 2014a, 2017, 2020; Leoné et al., 2015; Bosco et al., 2016; Piserchia et al., 2016; Cappadocia et al., 2017; De Vitis et al., 2019; Magri et al., 2019).

Distance representations in multiple reference frames across motor, premotor, and parietal reach nodes argue against a strict posterior-to-anterior gradient in sensorimotor transformations for skilled action, where posterior areas encode motor goals in gaze-centered reference frames and more anterior regions encode targets in body-centered reference frames. Previous studies have shown that both posterior and anterior regions within parietal and premotor areas integrate motor features in visual and proprioceptive coordinate space (Boussaoud et al., 1998; Buneo et al., 2002; Bernier and Grafton, 2010; Chang and Snyder, 2010; Bremner and Andersen, 2012; Hadjidimitrakis et al., 2014a; Piserchia et al., 2016). Thus, sensorimotor transformations might not be exclusively segregated along a posterior-to-anterior axis. If anything, our results give evidence for gaze- to body-centered transformations occurring temporally across multiple nodes of the dorsomedial reach pathway.

Most regions encoding distance information also encoded direction information independently during early planning, which, consistent with nonhuman primate work, suggests overlap in neuronal populations that encode direction and distance features critical for an upcoming goal-oriented reach (Messier and Kalaska, 2000; Churchland et al., 2006a; Hadjidimitrakis et al., 2014b, 2022; Bosco et al., 2016; Piserchia et al., 2016; De Vitis et al., 2019). Stronger representational specificity for direction than distance components during early planning and magnified distance representations in later planning support serial processing accounts showing that distance-related activity evolves more slowly than direction-related activity within premotor (Messier and Kalaska, 2000; Churchland et al., 2006a) and parietal regions (Hadjidimitrakis et al., 2014a,b, 2022; Piserchia et al., 2016). Critically, our results show that the human dorsomedial reach pathway is organized similarly, in that parameterizing the direction and distance of an upcoming reach action can be achieved by recruiting the same functional regions.

Heightened gaze- and body-centered representational specificity of a target's distance were seen in conjunction with a relative dissipation of direction-based representations during late planning. Many regions representing target positions (SPL 7pc, 7p, 5m, PMd caudal, M1) and hand positions (SPL 7pc, 7p, 5m, PMd rostral) during early planning more weakly encoded direction-based information during late planning. Unlike during early planning, magnified distance-representational specificity marginally exceeded direction-representational specificity across dorsomedial reach nodes. Stronger directional than distance encoding during early planning aligns with seminal PMd studies with nonhuman primates and more recent studies in parietal regions (Messier and Kalaska, 2000; Hadjidimitrakis et al., 2022). Similarly, transcranial magnetic stimulation in humans of caudal PMd near movement execution disrupts distance but not movement direction (Davare et al., 2015), which aligns with the relative dissipation of direction representations in caudal PMd observed here. Although direction-based representations relevant to an upcoming reach dissipated in late planning across the frontoparietal network, they were not completely absent. Hand and target position encoding persisted in three out of eight regions (hand, SPL 7a, 5l, M1; target, SPL 7a, 5l, PMd rostral), whereas representations of gaze position were mostly stable and invariant through early and late planning.

Our results are inconsistent with earlier nonhuman primate studies on direction and distance encoding that typically showed significant, and dominant, direction effects throughout the plan period (Messier and Kalaska, 2000; Churchland et al., 2006a). However, the strength and timing of preparatory activity is context dependent (Lara et al., 2018). In some nonhuman primate studies, the appearance of a spatial target cue evokes a transient directionally tuned burst of activity, which we have likely captured during our early planning epoch (when direction representations are heightened). This transient burst of activity can sometimes be followed by a sustained or decrementing directional signal at a lower level of discharge (Kalaska and Crammond, 1995; Crammond and Kalaska, 2000; Kaufman et al., 2014; Lara et al., 2018). This pattern of activity is often observed in tasks with long preparatory periods, similar to our design. The sustained lower level of discharge during a long preparatory period could explain the weaker direction encoding in late planning found here.

Further, sustained lower level directional signals still present during late planning might be undetected by our vRSA approach, which is set up to compare credible evidence for multiple distance and direction representations. In late planning, competing distance components are stronger than direction components. More recent monkey neurophysiology work that adopt similar paradigms show stronger distance than direction encoding consistent with our results (Hadjidimitrakis et al., 2022). Relatedly, planning a movement might generate a shift in population activity to drive the activity to an initial condition (e.g., direction; Churchland et al., 2006b). The shift toward this initial condition might be metabolically costly whereas its maintenance could be efficient. The net result would be strong direction-related BOLD activity patterns at the start of the delay period that are less evident later in the delay period even though the directional signal at the neural population activity level is maintained.

It is conceivable that representational specificity of a given movement parameter translates to accuracy and precision requirements of the task (Mahan and Georgopoulos, 2013; Rao and Donoghue, 2014; Barany et al., 2020). The requirement of the task used here placed a higher demand on distance (HT near, 2.3 cm; HT far, 4.6 cm) than direction (left and right targets spaced 180° apart). The differences in relative precision requirements may have necessitated sharper

representational encoding of distance near movement execution. In contrast, studies showing robust, sustained directional tuning typically employ tasks using more closely spaced targets (45°), which might demand sharper representational encoding of direction throughout the plan period (Messier and Kalaska, 2000; Churchland et al., 2006a; Fabbri et al., 2012).

Another task-related difference between our study and early nonhuman primate studies (Messier and Kalaska, 2000; Churchland et al., 2006a) is their lack of an explicit dissociation of eye position from hand/body position relative to upcoming reach targets as we have done here. Thus, it is unknown whether their observed neural activity scales with target direction relative to body or gaze coordinates. The extent to which PMd activity encodes eye positions is likely dependent on the task-specific constraints on eye position (Cisek and Kalaska, 2002). With our task design, we can interpret activity pattern differences between left- and right-sided targets to reflect varying target position representations in absolute space or relative to the hand or body. We show that absolute or body-centric target direction dissipated in later planning in caudal PMd.

Finally, and perhaps most importantly, our use of an ROI-based analysis of multivoxel patterns fundamentally differs from single-neuron or spike-rate histogram methods, where individual neurons or pockets of neurons may still encode for a specific feature (like direction) even as the broader population activity shifts to another feature (like distance). The fMRI vRSA approach captures population-level activity within the entire region and therefore may give a distinct perspective of the region's function and may account for the observed differences between our findings and work with nonhuman primates.

Nevertheless, we should be cautious in assuming that target direction effects are weaker during late-stage planning. For one, gaze position and target direction are necessarily coupled in our paradigm, and the strong gaze representations observed in many regions over time could be tied to the direction of the upcoming movement. It is important to qualify that gaze position representations persisted in caudal PMd (and other regions with target direction dissipation effects). These activity pattern differences between left- and right-sided gaze positions can reflect varying gaze positions in absolute space or relative to the hand, body, or target. In this way, gaze position effects may be partly driven by target direction differences relative to gaze. That all said, target direction representations persisted in SPL7a, 5l, and PMd rostral areas, in addition to widespread gaze representations. Given the fluidity of these representations over time, it is likely that regions including M1 represent this information after the go cue for accurate reaching. In line with this, Fabbri et al. (2012) showed during movement execution parietal encoding of direction and distance, consistent with what we show here during early and late planning (within 7a surveyed here). Similarly, they showed large to small adaptation in PMd suggesting nuanced amplitude encoding in direction-sensitive premotor areas.

Gaze fixation representations were widespread throughout the dorsomedial reach pathway and credibly evident across planning epochs, with large median Bayes factors. We caution against drawing major inferences relating to components with credible evidence with varying Bayes factor magnitudes, as our design was not set up to compare the size of component effects. Specifically, larger Bayes factor magnitudes for initial gaze fixation likely stem from contrasting activity patterns with greater positional differences between left and right gaze direction on the task board, than direction and distance differences contrasted in other components. It might have been more challenging to detect spatial activity differences between reaching toward left and right targets that are more closely spaced to each other than left and right gaze points. That said, previous fMRI studies have detected spatial activity pattern differences for left and right reach targets using similar or smaller directional and distance differences than that sampled here (Batista et al., 2007; Bernier and Grafton, 2010; Beurze et al., 2010; Fabbri et al., 2010, 2012). The narrow orientation of the hand and target buttons was selected to limit movement, allowing participants to reach from the hand to the target buttons without requiring movement of the entire arm. We also chose target and gaze positions ensuring that targets on all trials would always fall within an observer's near-peripheral zone within which there are little changes in visual acuity (Millodot et al., 1975; Larson and Loschky, 2009). In this way, we minimized between-condition activation pattern differences between near versus far distances between the gaze and target to be driven by visual acuity differences. Another methodological limitation of the current design is an inability to differentiate between anchor points for body-centered representations since hand-, shoulder-, and head-centered coordinate systems would be indistinguishable. Finally, with all movements executed along a single, horizontal axis, our results are specific to distance or movement amplitude in 2D (not 3D) space.

Encoding a goal in multiple reference frames supports the flexibility of the brain to convert or switch a target's distance, as well as its direction, relative to the gaze or body. These motor parameters (direction and distance) of an upcoming goal-directed reach can undergo sensorimotor transformations between gaze- and body-centric frames by recruiting the same areas. This aligns with the hypothesis that such transformations contribute to the brain's flexibility. Neuronal encoding of motor parameters in multiple coordinate frames, as demonstrated in our study, supports computational models emphasizing the flexibility, efficiency, and power of individual nodes coding diverse inputs to optimally combine or transform extrinsic or intrinsic representations (Körding and Wolpert, 2004; Sober and Sabes, 2005; McGuire and Sabes, 2009).

Brain–computer interface technology decoding motor intention through neural activity for generating movement goals has advanced rapidly with the integration of sensory information (Flesher et al., 2021). Harnessing sensorimotor integration's benefits requires carefully delineating the timing and reference frame in which multiple motor parameters are specified for goal-directed action. Representations of direction and distance in multiple reference frames observed here are consistent with computational models specifying a flexible brain that can anchor motor parameters to the most reliable or task-applicable sensory source. Future work should clarify how sensorimotor transformations within and between

motor parameters unfold with uncertainty in the neural circuitry supporting goal-directed action, with sensorimotor declines present in many neurological disorders at birth (Bleyenheuft and Gordon, 2013; Gupta et al., 2017) and later in life (Abbruzzese and Berardelli, 2003), including healthy aging (Cham et al., 2007; Seidler et al., 2010; Kuehn et al., 2018; Cassady et al., 2020). The present study's task-based fMRI approach with pattern component modeling contributes to closing a critical divide between nonhuman and human neurophysiology by characterizing how and when goal-relevant representations for upcoming action are encoded.

References

Abbruzzese G, Berardelli A (2003) Sensorimotor integration in movement disorders. Mov Disord 18:231–240.

Amunts K, Mohlberg H, Bludau S, Zilles K (2020) Julich-Brain: a 3D probabilistic atlas of the human brain's cytoarchitecture. Science 369:988–992.

Andersen RA, Buneo CA (2002) Intentional maps in posterior parietal cortex. Annu Rev Neurosci 25:189–220.

Ariani G, Oosterhof NN, Lingnau A (2018) Time-resolved decoding of planned delayed and immediate prehension movements. Cortex 99:330–345.

Ariani G, Pruszynski JA, Diedrichsen J (2022) Motor planning brings human primary somatosensory cortex into action-specific preparatory states. Elife 11:e69517.

Barany DA, Della-Maggiore V, Viswanathan S, Cieslak M, Grafton ST (2014) Feature interactions enable decoding of sensorimotor transformations for goal-directed movement. J Neurosci 34:6860–6873.

Barany DA, Revill KP, Caliban A, Vernon I, Shukla A, Sathian K, Buetefisch CM (2020) Primary motor cortical activity during unimanual movements with increasing demand on precision. J Neurophysiol 124:728–739.

Bastian A, Schöner G, Riehle A (2003) Preshaping and continuous evolution of motor cortical representations during movement preparation. Eur J Neurosci 18:20472058.

Batista AP, Buneo CA, Snyder LH, Andersen RA (1999) Reach plans in eye-centered coordinates. Science 285:257–260.

Batista AP, Santhanam G, Yu BM, Ryu SI, Afshar A, Shenoy KV (2007) Reference frames for reach planning in macaque dorsal premotor cortex. J Neurophysiol 98:966–983.

Battaglia-Mayer A, Caminiti R, Lacquaniti F, Zago M (2003) Multiple levels of representation of reaching in the parieto-frontal network. Cereb Cortex 13:1009–1022.

Bernier P-M, Grafton ST (2010) Human posterior parietal cortex flexibly determines reference frames for reaching based on sensory context. Neuron 68:776–788.

Beurze SM, Toni I, Pisella L, Medendorp WP (2010) Reference frames for reach planning in human parietofrontal cortex. J Neurophysiol 104:1736–1745.

Bleyenheuft Y, Gordon AM (2013) Precision grip control, sensory impairments and their interactions in children with hemiplegic cerebral palsy: a systematic review. Res Dev Disabil 34:3014–3028.

Bosco A, Breveglieri R, Hadjidimitrakis K, Galletti C, Fattori P (2016) Reference frames for reaching when decoupling eye and target position in depth and direction. Sci Rep 6:21646.

Boussaoud D, Jouffrais C, Bremmer F (1998) Eye position effects on the neuronal activity of dorsal premotor cortex in the macaque monkey. J Neurophysiol 80:1132–1150.

Bremner LR, Andersen RA (2012) Coding of the reach vector in parietal area 5d. Neuron 75:342–351.

Buneo CA, Jarvis MR, Batista AP, Andersen RA (2002) Direct visuomotor transformations for reaching. Nature 416:632–636.

Cappadocia DC, Monaco S, Chen Y, Blohm G, Crawford JD (2017) Temporal evolution of target representation, movement direction planning, and reach execution in occipital–parietal–frontal cortex: an fMRI study. Cereb Cortex 27:5242–5260.

Casey BJ, Cannonier T, Conley MI, Cohen AO, Barch DM, Heitzeg MM, Soules ME, Teslovich T, Dellarco DV, Garavan H (2018) The adolescent brain cognitive development (ABCD) study: imaging acquisition across 21 sites. Dev Cogn Neurosci 32:43–54.

Cassady K, Ruitenberg MFL, Reuter-Lorenz PA, Tommerdahl M, Seidler RD (2020) Neural dedifferentiation across the lifespan in the motor and somatosensory systems. Cereb Cortex 30:3704–3716.

Cham R, Perera S, Studenski SA, Bohnen NI (2007) Striatal dopamine denervation and sensory integration for balance in middle-aged and older adults. Gait Posture 26:516–525.

Chang SW, Snyder LH (2010) Idiosyncratic and systematic aspects of spatial representations in the macaque parietal cortex. Proc Natl Acad Sci U S A 107:7951–7956.

Churchland MM, Byron MY, Ryu SI, Santhanam G, Shenoy KV (2006b) Neural variability in premotor cortex provides a signature of motor preparation. J Neurosci 26:3697–3712.

Churchland MM, Santhanam G, Shenoy KV (2006a) Preparatory activity in premotor and motor cortex reflects the speed of the upcoming reach. J Neurophysiol 96:3130–3146.

Cisek P, Kalaska JF (2002) Modest gaze-related discharge modulation in monkey dorsal premotor cortex during a reaching task performed with free fixation. J Neurophysiol 88:1064–1072.

Coallier É, Michelet T, Kalaska JF (2015) Dorsal premotor cortex: neural correlates of reach target decisions based on a color-location matching rule and conflicting sensory evidence. J Neurophysiol 113:3543–3573.

Crammond DJ, Kalaska JF (2000) Prior information in motor and premotor cortex: activity during the delay period and effect on premovement activity. J Neurophysiol 84:986–1005.

Crawford JD, Henriques DY, Medendorp WP (2011) Three-dimensional transformations for goal-directed action. Annu Rev Neurosci 34:309–331.

Cross ES, Schmitt PJ, Grafton ST (2007) Neural substrates of contextual interference during motor learning support a model of active preparation. J Cogn Neurosci 19:1854–1871.

Davare M, Zénon A, Desmurget M, Olivier E (2015) Dissociable contribution of the parietal and frontal cortex to coding movement direction and amplitude. Front Hum Neurosci 9:241.

Davare M, Zenon A, Pourtois G, Desmurget M, Olivier E (2012) Role of the medial part of the intraparietal sulcus in implementing movement direction. Cereb Cortex 22:1382–1394.

Denyer R, Greenhouse I, Boyd LA (2022) The role of PMd in voluntary motor control: insights from TMS research.

De Vitis M, Breveglieri R, Hadjidimitrakis K, Vanduffel W, Galletti C, Fattori P (2019) The neglected medial part of macaque area PE: segregated processing of reach depth and direction. Brain Struct Funct 224:2537–2557.

Diedrichsen J, Shadmehr R (2005) Detecting and adjusting for artifacts in fMRI time series data. Neuroimage 27:624–634.

Dubois J, de Berker AO, Tsao DY (2015) Single-unit recordings in the macaque face patch system reveal limitations of fMRI MVPA. J Neurosci 35:2791–2802.

Fabbri S, Caramazza A, Lingnau A (2010) Tuning curves for movement direction in the human visuomotor system. J Neurosci 30:13488–13498.

Fabbri S, Caramazza A, Lingnau A (2012) Distributed sensitivity for movement amplitude in directionally tuned neuronal populations. J Neurophysiol 107:1845–1856.

Fabbri S, Strnad L, Caramazza A, Lingnau A (2014) Overlapping representations for grip type and reach direction. Neuroimage 94:138–146.

Fan L, Li H, Zhuo J, Zhang Y, Wang J, Chen L, Yang Z, Chu C, Xie S, Laird AR (2016) The human brainnetome atlas: a new brain atlas based on connectional architecture. Cereb cortex 26:3508–3526.
Fiehler K, Karimpur H (2023) Spatial coding for action across spatial scales. Nat Rev Psychol 2:72–84.
Flesher SN, Downey JE, Weiss JM, Hughes CL, Herrera AJ, Tyler-Kabara EC, Boninger ML, Collinger JL, Gaunt RA (2021) A brain-computer interface that evokes tactile sensations improves robotic arm control. Science 372:831–836.
Fooken J, Baltaretu BR, Barany DA, Diaz G, Semrau JA, Singh T, Crawford JD (2023) Perceptual-cognitive integration for goal-directed action in naturalistic environments. J Neurosci 43:7511–7522.
Friston KJ, Diedrichsen J, Holmes E, Zeidman P (2019) Variational representational similarity analysis. Neuroimage 201:115986.
Galletti C, Fattori P, Kutz DF, Battaglini PP (1997) Arm movement-related neurons in the visual area V6A of the macaque superior parietal lobule. Eur J Neurosci 9:410–413.
Gallivan JP, Cavina-Pratesi C, Culham JC (2009) Is that within reach? fMRI reveals that the human superior parieto-occipital cortex encodes objects reachable by the hand. J Neurosci 29:4381–4391.
Gallivan JP, McLean A, Culham JC (2011a) Neuroimaging reveals enhanced activation in a reach-selective brain area for objects located within participants' typical hand workspaces. Neuropsychologia 49:3710–3721.
Gallivan JP, McLean DA, Valyear KF, Pettypiece CE, Culham JC (2011b) Decoding action intentions from preparatory brain activity in human parieto-frontal networks. J Neurosci 31:9599–9610.
Gelman A, Hill J, Yajima M (2012) Why we (usually) don't have to worry about multiple comparisons. J Res Educ Eff 5:189–211.
Gelman A, Loken E (2016) The statistical crisis in science. In: *The best writing on mathematics* (Pitici M, ed), pp 305–318. Princeton, NJ: Princeton University Press.
Glasser MF, Coalson TS, Robinson EC, Hacker CD, Harwell J, Yacoub E, Ugurbil K, Andersson J, Beckmann CF, Jenkinson M (2016) A multi-modal parcellation of human cerebral cortex. Nature 536:171–178.
Gordon J, Ghilardi MF, Ghez C (1994) Accuracy of planar reaching movements: I. Independence of direction and extent variability. Exp Brain Res 99:97–111.
Graziano MS, Gross CG (1998) Spatial maps for the control of movement. Curr Opin Neurobiol 8:195–201.
Gupta D, Barachant A, Gordon AM, Ferre C, Kuo HC, Carmel JB, Friel KM (2017) Effect of sensory and motor connectivity on hand function in pediatric hemiplegia. Ann Neurol 82:766–780.
Hadjidimitrakis K, Bertozzi F, Breveglieri R, Bosco A, Galletti C, Fattori P (2014b) Common neural substrate for processing depth and direction signals for reaching in the monkey medial posterior parietal cortex. Cereb Cortex 24:1645–1657.
Hadjidimitrakis K, Bertozzi F, Breveglieri R, Fattori P, Galletti C (2014a) Body-centered, mixed, but not hand-centered coding of visual targets in the medial posterior parietal cortex during reaches in 3D space. Cereb Cortex 24:3209–3220.
Hadjidimitrakis K, Bertozzi F, Breveglieri R, Galletti C, Fattori P (2017) Temporal stability of reference frames in monkey area V6A during a reaching task in 3D space. Brain Struct Funct 222:1959–1970.
Hadjidimitrakis K, De Vitis M, Ghodrati M, Filippini M, Fattori P (2022) Anterior-posterior gradient in the integrated processing of forelimb movement direction and distance in macaque parietal cortex. Cell Rep 41:1–13.
Hadjidimitrakis K, Ghodrati M, Breveglieri R, Rosa MG, Fattori P (2020) Neural coding of action in three dimensions: task-and time-invariant reference frames for visuospatial and motor-related activity in parietal area V6A. J Comp Neurol 528:3108–3122.
Johnson SH, Grafton ST (2003) From 'acting on' to 'acting with': the functional anatomy of object-oriented action schemata. Prog Brain Res 142:127–139.
Kalaska JF, Crammond DJ (1995) Deciding not to GO: neuronal correlates of response selection in a GO/NOGO task in primate premotor and parietal cortex. Cereb Cortex 5:410–428.
Kassner M, Patera W, Bulling A (2014) Pupil: an open source platform for pervasive eye tracking and mobile gaze-based interaction. In: *Proceedings of the 2014 ACM international joint conference on pervasive and ubiquitous computing: adjunct publication* (UbiComp '14 Adjunct), pp 1151–1160. New York, NY: Association for Computing Machinery.
Kaufman MT, Churchland MM, Ryu SI, Shenoy KV (2014) Cortical activity in the null space: permitting preparation without movement. Nat Neurosci 17:440–448.
Kaufman MT, Churchland MM, Santhanam G, Yu BM, Afshar A, Ryu SI, Shenoy KV (2010) Roles of monkey premotor neuron classes in movement preparation and execution. J Neurophysiol 104:799–810.
Körding KP, Wolpert DM (2004) Bayesian integration in sensorimotor learning. Nature 427:244–247.
Kreter N, Dundon NM, Smith J, Marneweck M (2024) Sensory context of initiation-cue modulates action goal-relevant neural representations. bioRxiv:2024.2009.2003.611077.
Kruschke J (2014) *Doing Bayesian data analysis: a tutorial withR, JAGS, and Stan*, Ed 2. London, UK: Elsevier.
Kuehn E, Perez-Lopez MB, Diersch N, Döhler J, Wolbers T, Riemer M (2018) Embodiment in the aging mind. Neurosci Biobehav Rev 86:207–225.
Lara AH, Elsayed GF, Zimnik AJ, Cunningham JP, Churchland MM (2018) Conservation of preparatory neural events in monkey motor cortex regardless of how movement is initiated. Elife 7: e31826.
Larson AM, Loschky LC (2009) The contributions of central versus peripheral vision to scene gist recognition. J Vis 9:6–6.
Leoné FT, Monaco S, Henriques DY, Toni I, Medendorp WP (2015) Flexible reference frames for grasp planning in human parietofrontal cortex. eNeuro 2:1–15.
Magri C, Fabbri S, Caramazza A, Lingnau A (2019) Directional tuning for eye and arm movements in overlapping regions in human posterior parietal cortex. Neuroimage 191:234–242.
Mahan MY, Georgopoulos AP (2013) Motor directional tuning across brain areas: directional resonance and the role of inhibition for directional accuracy. Front Neural Circuits 7:92.
Marneweck M, Gardner C, Dundon NM, Smith J, Frey SH (2023) Reorganization of sensorimotor representations of the intact limb after upper but not lower limb traumatic amputation. Neuroimage Clin 39:103499.
Marneweck M, Grafton ST (2020a) Neural substrates of anticipatory motor adaptation for object lifting. Sci Rep 10:1–10.
Marneweck M, Grafton ST (2020b) Overt and covert object features mediate timing of patterned brain activity during motor planning. Cereb Cortex Commun 1:tgaa080.
Marneweck M, Grafton ST (2020c) Representational neural mapping of dexterous grasping before lifting in humans. J Neurosci 40:2708–2716.
Marzocchi N, Breveglieri R, Galletti C, Fattori P (2008) Reaching activity in parietal area V6A of macaque: eye influence on arm activity or retinocentric coding of reaching movements? Eur J Neurosci 27:775–789.
McGuire LM, Sabes PN (2009) Sensory transformations and the use of multiple reference frames for reach planning. Nat Neurosci 12:1056–1061.
Messier J, Kalaska J (1997) Differential effect of task conditions on errors of direction and extent of reaching movements. Exp Brain Res 115:469–478.
Messier J, Kalaska JF (2000) Covariation of primate dorsal premotor cell activity with direction and amplitude during a memorized-delay reaching task. J Neurophysiol 84:152–165.
Millodot M, Johnson CA, Lamont A, Leibowitz HW (1975) Effect of dioptrics on peripheral visual acuity. Vision Res 15:1357–1362.
Moeller S, Yacoub E, Olman CA, Auerbach E, Strupp J, Harel N, Uğurbil K (2010) Multiband multislice GE-EPI at 7 tesla, with 16-fold acceleration using partial parallel imaging with application to high spatial and temporal whole-brain fMRI. Magn Reson Med 63:1144–1153.

Pesaran B, Nelson MJ, Andersen RA (2006) Dorsal premotor neurons encode the relative position of the hand, eye, and goal during reach planning. Neuron 51:125–134.
Pisella L, Sergio L, Blangero A, Torchin H, Vighetto A, Rossetti Y (2009) Optic ataxia and the function of the dorsal stream: contributions to perception and action. Neuropsychologia 47:3033–3044.
Piserchia V, Breveglieri R, Hadjidimitrakis K, Bertozzi F, Galletti C, Fattori P (2016) Mixed body/hand reference frame for reaching in 3D space in macaque parietal area PEc. Cereb Cortex 27:1976–1990.
Pouget A, Ducom JC, Torri J, Bavelier D (2002) Multisensory spatial representations in eye-centered coordinates for reaching. Cognition 83:B1–B11.
Rao NG, Donoghue JP (2014) Cue to action processing in motor cortex populations. J Neurophysiol 111:441–453.
Rizzolatti G, Matelli M (2003) Two different streams form the dorsal visual system: anatomy and functions. Exp Brain Res 153:146–157.
Seidler RD, Bernard JA, Burutolu TB, Fling BW, Gordon MT, Gwin JT, Kwak Y, Lipps DB (2010) Motor control and aging: links to age-related brain structural, functional, and biochemical effects. Neurosci Biobehav Rev 34:721733.
Setsompop K, Gagoski BA, Polimeni JR, Witzel T, Wedeen VJ, Wald LL (2012) Blipped-controlled aliasing in parallel imaging for simultaneous multislice echo planar imaging with reduced g-factor penalty. Magn Reson Med 67:1210–1224.
Sober SJ, Sabes PN (2005) Flexible strategies for sensory integration during motor planning. Nat Neurosci 8:490–497.
Turella L, Rumiati R, Lingnau A (2020) Hierarchical action encoding within the human brain. Cereb Cortex 30:2924–2938.
Vindras P, Desmurget M, Viviani P (2005) Error parsing in visuomotor pointing reveals independent processing of amplitude and direction. J Neurophysiol 94:1212–1224.
Wise S, Mauritz K-H (1985) Set-related neuronal activity in the premotor cortex of rhesus monkeys: effects of changes in motor set. Proc R Soc Lond B Biol Sci 223:331–354.
Yewbrey R, Mantziara M, Kornysheva K (2023) Cortical patterns shift from sequence feature separation during planning to integration during motor execution. J Neurosci 43:1742–1756.